Detrital U-Pb zircon and $^{40}Ar/^{39}Ar$ muscovite geochronology from Middle Pennsylvanian strata in the Anadarko Basin, Texas Panhandle, USA

R. Spencer Hollingworth[1], Ryan J. Leary[1], Matthew T. Heizler[1,2]

[1]Department of Earth and Environmental Science, New Mexico Institute of Mining and Technology, Socorro, NM, USA

[2]New Mexico Bureau of Geology and Mineral Resources, New Mexico Institute of Mining and Technology, Socorro, NM, USA

Email Addresses:

R. Spencer Hollingworth: shollingworth1722@gmail.com (corresponding author)

Ryan J. Leary: ryan.leary@nmt.edu

Matthew T. Heizler: Matt.Heizler@nmt.edu

Keywords: Amarillo-Wichita Uplift; Ancestral Rocky Mountains; Sierra Grande Uplift; Laurentia; Desmoinesian; Morrowan

Abstract

The Late Mississippian-Permian Anadarko Basin formed in Texas and Oklahoma, USA as the result of inversion of Neoproterozic and Cambrian rift structures. Subsidence was driven by flexural loading of the Amarillo-Wichita Uplift, and this uplift may represent the easternmost element of the Ancestral Rocky Mountains system. The northwestern part of this basin has generally been interpreted to have been filled by sediment derived from the Ancestral Front Range Uplift, ~475 km to the northwest during the early stages of basin filling. We test this model using U-Pb detrital zircon and $^{40}Ar/^{39}Ar$ detrital muscovite results from three subsurface samples of the Morrow B sandstone in the northwestern part of the Anadarko Basin. We provide a new maximum depositional age of 310.9 ± 4.9 Ma that indicates the age of the Morrow B to be no older than late Atokan to early Desmoinesian Age (Moscovian), ~10 Myr younger than previously interpreted. In contrast to some previous interpretations, we propose that the most likely source for the sediment in the Morrow B is the Amarillo Uplift to the south. Detrital zircon and detrital muscovite data have age peaks at 900-1300 Ma, 1370 Ma and 1600-1800 Ma corresponding to derivation from Grenville, Granite-Rhyolite and Yavapai-Mazatzal basement provinces, respectively. A dominant detrital zircon peak at 1370 Ma suggests that Mesoproterozoic granites in the Amarillo Uplift were exposed by Middle Pennsylvanian time, and detritus eroded from the Amarillo Uplift dominated the lowstand sediment budget of the Texas Panhandle during this time; small volumes of sediment were likely sourced from the Ancestral Front Range. This study presents the first detrital geochronology data from the subsurface Anadarko Basin and the first detrital muscovite data from late Paleozoic southwestern Laurentia. The results presented here highlight the interpretive power of combined detrital zircon and muscovite datasets.

1. Introduction

The collision between the Laurentian and Gondwanan continents along the Ouachita-Marathon Fold Belt led, at least in part, to a series of major uplifts, including the Ancestral Rocky Mountains and the Amarillo-Wichita Uplift and their associated basins: the Denver, Paradox, Eagle, and Anadarko basins (Fig. 1). The Ancestral Rocky Mountains uplifts, which were made up of multiple geographic highs, formed in an intra-plate setting, and numerous models have been proposed for their origin including: stress from the Ouachita-Marathon Belt (Kluth and Coney, 1981; Dickinson and Lawton, 2001), reactivation of preexisting basement faults (Marshak et al., 2000), flat-slab subduction along the Sonoran margin of southwestern Laurentia (Ye et al., 1996), dynamic uplift/subsidence associated with Cambrian mafic underplating (Soreghan et al., 2012), or a combination of plate interactions along the Sonoran, Nevadan, and Ouachita-Marathon margins (Leary et al., 2017). Whether deformation and uplift of the Amarillo-Wichita Uplift were driven by the same processes that drove deformation and uplift in the Ancestral Rocky Mountains remains poorly understood. Many workers have interpreted collision along the Ouachita-Marathon Belt to have driven compressional deformation of the Amarillo-Wichita Uplift (Fig. 1; Kluth and Coney, 1981; Budnik, 1986; Soreghan et al., 2012), but others have interpreted deformation as the result of stress generated along the southwestern Laurentian margin (Ye et al., 1996; Leary et al., 2017). If the Ancestral Rocky Mountains and the Amarillo-Wichita Uplift were uplifted by the same forces, then the Amarillo-Wichita would represent the earliest and easternmost expression of Ancestral Rocky Mountains deformation (e.g. Soreghan et al., 2012) .

Detrital mineral provenance studies across the Ancestral Rocky Mountains orogen suggest that exhumation of Ancestral Rocky Mountains uplifts began by at least the Atokan Age (Bashkirian-Moscovian). The Denver, Eagle, and Paradox basins were primarily filled by Ancestral Rocky Mountains detritus with minor components of far-traveled sediment from a variety of sources (Leary et al., 2020a; Leary et al., 2020b). Although the Anadarko Basin was the earliest possibly Ancestral Rocky Mountains-related basin to begin accumulating syn-tectonic sediment (Soreghan et al., 2012), no detrital geochronology studies have sampled Pennsylvanian-lower Permian syn-tectonic strata within the Anadarko Basin (Thomas et al., 2016; 2019). As such, the relative contribution of Amarillo-Wichita-sourced sediment versus extra-basinal sediment is unknown for the most active stage of Anadarko Basin subsidence

(Soreghan et al., 2012). Here, we present the first detrital mineral geochronology study of Lower Pennsylvanian subsurface strata in the Anadarko Basin directly testing the timing and contribution of adjacent Amarillo-Wichita detritus to the basin. This study also refines the age of the Morrow B sandstone to Desmoinesian (Moscovian) Age by establishing a new maximum depositional age.

Radioisotopic dating of detrital minerals such as zircon, sanidine, biotite, and muscovite for provenance studies has been a key tool in reconstructing paleogeography and sediment routing in a wide range of depositional systems (e.g. Gehrels et al., 2011; Blum and Pecha, 2014; Mulder et al., 2017; Benowitz et al., 2019; Cather et al., 2019; Leary et al., 2020b). Although single mineral geochronometers have yielded powerful provenance datasets, the combining of multiple geochronometers has the potential to capture a much wider range of crystallization and/or cooling temperatures in sediment source areas (e.g. Gutiérrez-Alonso et al., 2005; Mulder et al., 2017). Multiple geochronometers can also account for variable mineral fertility across source lithologies (e.g. Moecher and Samson, 2006; Repasch et al., 2017) and variable hydrodynamic properties during sediment transport (Garzanti et al., 2008; Resentini et al., 2013; Augustsson et al., 2019). Therefore, multiple detrital geochronometers can provide a more comprehensive interpretation of paleogeography, sediment routing, and sediment recycling. The data presented here provide an important example of the power of combining detrital geochronometers from opposite ends of the hydrodynamic spectrum (Garzanti et al., 2008; Resentini et al., 2013) and highlight the advantage of multiple provenance indicators.

This study presents detrital zircon U-Pb and detrital muscovite $^{40}Ar/^{39}Ar$ data from Middle Pennsylvanian strata known locally as the Morrow B (Ampomah et al., 2016) or Morrow Buckhaults (Munson, 1989) (Fig. 2), in the northwestern part of the Anadarko Basin (Ochiltree county, Texas, USA). Samples were collected from three drill cores in an oilfield known as the Farnsworth Unit made available through a Department of Energy funded carbon capture utilization and storage case-study called the Southwest Regional Partnership on Carbon Sequestration (SWP).

2. Geologic background

The Southern Oklahoma Aulacogen formed during the Neoproterozoic to Cambrian as a failed rift arm during the breakup of the Rodinian supercontinent ca. 860-750 Ma (Perry, 1989; Keller and Stephenson, 2007; Li et al., 2008). Subsidence in the Southern Oklahoma Aulacogen was driven by thermal subsidence following intrusion of middle Cambrian igneous rocks. Thermal subsidence persisted in the surrounding area until the Early Mississippian (Feinstein, 1981; Perry, 1989; Soreghan et al., 2012). Beginning during the Late Mississippian, progressive closure of the Rheic Ocean and collision between Gondwana and Laurentia drove deformation and subsidence of a series of basins along the Laurentian margin including the Black Warrior, Arkoma, Ardmore, Fort Worth, Val Verde, and Marfa basins (Graham et al., 1975; Ross, 1986; Dickinson and Lawton, 2003; Alsalem et al., 2017).

Rapid subsidence in the Anadarko Basin began in Late Mississippian time as the result of flexural loading by deformation along the Amarillo-Wichita Uplift (Johnson, 1989; Perry, 1989; Soreghan et al., 2012). Similar patterns of uplift and subsidence occurred throughout the Ancestral Rocky Mountains province in the Denver, Eagle, and Paradox basins, although subsidence in those basins did not begin until Early Pennsylvanian (Ye et al., 1996; Dickinson and Lawton, 2001; Leary et al., 2017); and basement exhumation in most Ancestral Rocky Mountain uplifts did not occur until the Middle Pennsylvanian (Gehrels et al., 2011; Leary et al., 2020b).

During the Pennsylvanian and Permian, southwestern Laurentia was located at equatorial latitudes, whereas Gondwana was located at more southerly latitudes (Scotese et al., 1999; Domeier and Torsvik, 2014). High-frequency fluctuations between glacial and interglacial conditions caused high-frequency fluctuation in eustacy , although interpretations of the magnitude of sea-level change vary from < 50 m to > 100 m (Ross and Ross, 1987; Heckel, 2008). Bowen and Weimer (2003) attribute ~280 km of lateral shoreline displacement in the American midcontinent to this sea-level change during the Early Pennsylvanian.

The Morrow B sandstone is a coarse-grained sandstone preserved in the northwest corner of the Anadarko Basin (northern Texas panhandle). Within the study area, the Morrow B is a 10.2-15.9 m (33.5-52.3 ft) thick medium-grained sandstone to pebble conglomerate. The base of the unit is a 30-90 cm (1 to 3 ft) thick, matrix-supported conglomerate with clasts up to 5 cm (2 in) in diameter. The conglomerate overlies a sharp, erosional surface with the underlying Morrow Shale (Figs. 3-4). Facies associations include massive, laminated, and cross-bedded sandstones and conglomerates, with stylolites and clay seams (Fig. 3-4; Rose-Coss, 2017). Rose-Coss (2017) used Ultra-Sonic Borehole Images logs to determine that planar features in the core dip between 20-30° to the east-northeast, and he interpreted dip directions to reflect fluvial cross strata and thus sediment transport direction.

The Morrow B consists of a NW-SE trending sandstone belt incised into marine shales. This stratigraphic juxtaposition along with the Morrow B's sharp basal contact, basal conglomerate, cross-bedded sandstones, and clay seams/drapes, has been interpreted to represent fluvial deposition within an incised valley with tidal influence (Gallagher, 2014; Rose-Coss, 2017). Siltstone facies that overlie the fluvial sandstones have been interpreted as being deposited in an estuarine setting (Gallagher, 2014; Rose-Coss, 2017). Pennsylvanian deposits with similar architecture in southeastern Colorado have also been interpreted as incised valleys (Bowen and Weimer, 2003; Puckett et al., 2008).

3. Materials and methods

3.1 Detrital zircon analysis

Four samples were collected from the Farnsworth field Morrow B sandstone and the B1 sandstone, a lower sand interval intersected by well 32-8 (Fig. 3). One sample each was collected from wells 13-10A at 2343.3 m (7688 ft) and 13-14 at 2351.5 m (7715 ft) and two samples were collected from well 32-8 at 2426.5 m (7961 ft) and 2445.4 m (8023 ft) (Fig. 3; Table 1). Samples were named based on well name and depth in feet. Samples were processed at ZirChron LLC and were separated by Electro Pulse Disaggregator, which applies a strong electric field to the rock while submerged underwater in order to break the rock down along existing grain boundaries. A water table and heavy liquids were used to separate grains by density, and a Frantz magnetic separator removed magnetic minerals from the remaining grains. Three of the four samples yielded zircons grains: 13-10A-7688, 13-14-7715, and 32-8-7961; whereas sample 32-8-8023 did not (Fig. 3). All samples were analyzed at the University of Arizona LaserChron Center. There, zircon grains were mounted in epoxy with zircon standards, polished, and then imaged using the Hitachi 3400N Scanning Electron Microscope. Grains were analyzed by U-Pb laser ablation multicollector inductively coupled plasma mass spectrometer (LA-MC-ICPMS) (Gehrels et al., 2006; Gehrels et al., 2008). We analyzed 132 grains from sample 13-10A-7688, 318 grains from sample 13-14-7715, and 351 grains from sample 32-8-7961. See supplemental Data Table 1 for analytical settings. During analysis, zircon grains were ablated using a Photon Machines Analyte G2 excimer laser with a spot diameter of 30 µm. For each analysis, the errors in determining $^{206}Pb/^{238}U$ and $^{206}Pb/^{204}Pb$ result in a measurement error of ~1-2% (at 2σ level) in the $^{206}Pb/^{238}U$ age. The errors in measurement of $^{206}Pb/^{207}Pb$ and $^{206}Pb/^{204}Pb$ also result in ~1-2% (at 2σ level) uncertainty in age for grains that are >1.0 Ga, but are substantially larger for younger grains due to low intensity of the ^{207}Pb signal. Apparent ages were filtered using 25% discordance and 5% reverse-discordance.

3.2 Detrital muscovite analysis

A portion of the 32-8-7961 sample was crushed, washed, and sieved between the No. 20-60 mesh (841-250 μm), before hand picking 50-75 detrital muscovite crystals. Optical inspection under a binocular microscope and the very high K/Ca values (determined from $^{39}Ar/^{37}Ar$) indicate that the crystals are devoid of Ca and thus do not have smectitic or other clay alteration. Crystals were irradiated at the Oregon State Triga reactor for 14 hours in the NM-309 package. The flux monitor used during irradiation was Fish Canyon Tuff dated to 28.201 ± 0.046 Ma (Kuiper et al., 2008). A decay constant of $5.463e^{-10}$ /yr was used in age calculations (Min et al., 2000). Due to large analytical time and cost, 30 of the 50-75 crystals were dated. Crystals were step heated in 7 to 16 increments using a Photon Machines CO_2 laser and gas was measured using the Argus VI mass spectrometer at the New Mexico Geochronology Research Laboratory at the New Mexico Bureau of Geology and Mineral Resources. Plateau ages were calculated for most of the age spectra and represent the inverse variance weighted mean of the selected steps. The closure temperature of muscovite varies based on crystal size and cooling rate and we use a nominal closure temperature of ~400°C for this study (Harrison et al., 2009).

4. Results

4.1 Detrital zircon

Sample 13-10A-7688 yielded 128 concordant ages from a total of 132 ages; sample 13-14-7715 yielded 306 concordant ages from a total of 318 ages; sample 32-8-7961 yielded 341 concordant ages from a total of 351 ages. Detrital zircon age distributions are shown by probability density plots and kernel density estimates with a bandwidth of 20 Myr (Fig. 5); histograms in each plot have 50 Myr bin width. Spectra in each sample are dominated by a primary peak centered at 1370 Ma, and grains in this population make up more than 50% of each sample. To better illustrate subordinate peaks, the above plots are also constructed following removal of the prominent 1370 Ma peak (Fig. 5B). All samples also contain peaks in the age ranges of 1900-1625 Ma, 1500-1400 Ma, and 1300-900 Ma. In addition, sample 13-10A-7688 has peaks at 2740 Ma, 520 Ma, and 430 Ma; 13-14-7715 has age peaks at 2740 Ma, 2650 Ma, 620 Ma, 450 Ma, and 310 Ma; and 32-8-7961 has peaks at 650 Ma, 580 Ma, 480 Ma, and 420 Ma. A maximum depositional age of 310.9 ± 4.9 Ma (MSWD = 2.1, n = 3) was calculated based on the youngest grains for sample 13-14-7715 with Isoplot (Ludwig, 2003), using a weighted average at 2σ (Fig. 6).

4.2 Detrital muscovite

Detrital muscovite grains were recovered from sample 32-8-7961, from which 30 plateau ages were obtained ranging from 1644 Ma to 1215 Ma (Fig. 7). Step-heating age spectra commonly show late Precambrian initial steps that climb steeply to overall flat segments referred to as plateaus. These plateau segments commonly have > 5 steps comprising >60% of the ^{39}Ar released, but in some instances are represented by less gas and fewer steps. The plateau age errors are reported to 1σ and range from 1.6 Ma to 16.2 Ma. Plateau ages are presented in probability density plots and kernel density estimates with a bandwidth of 20 Ma. Spectra of muscovite ages shows a tri-modal age distribution with major peaks at 1230, 1370, and 1620 Ma (Fig. 5A).

5. Discussion

5.1 Morrow B depositional age

The Morrow B sandstone has previously been reported to fall within the Morrowan Age (Bashkirian) (Munson, 1989; Ampomah et al., 2016). Near-depositional age grains dated from sample 13-14-7715 provide the first radioisotopic age for the Morrow B sandstone. The newly calculated maximum depositional age of 310.9 ± 4.9 Ma (Fig. 6) shifts the Morrow B from Morrowan to late Atokan or early Desmoinesian (Moscovian) Age (Richards, 2013). The previous age determination for the Morrow B was based on biostratigraphic dating of the Thirteen Finger Limestone, which overlies the Morrow (Fig. 2; Rascoe and Adler, 1983). However, the biostratigraphy is based on the presence of *Fusulinella*, which indicates an age from late Atokan (Moscovian) to early Desmoinesian (Moscovian) (Wahlman, 2013). Thus, depending on sedimentation rates, both the Morrow B and the Thirteen Finger Limestone could be Desmoinesian (Moscovian-Kasimovian) Age. Furthermore, biostratigraphic ages used to determine the age for the Thirteen Finger Limestone in the study area come from southern Colorado (Maher, 1948) and Kansas (Lee, 1953), approximately 250 and 150 km away from the current study area, respectively. Thirteen Finger Limestone strata in Colorado and Kansas may not be time correlative with the Thirteen Finger Limestone in the Texas Panhandle. Therefore, we argue that the newly calculated radioisotopic age is a robust maximum allowable age for the Morrow B sandstone in the Texas Panhandle.

5.2 Possible zircon sources

Zircon age spectra that appear to have nearly unimodal age distributions such as those presented in Fig. 5A are often interpreted to indicate proximal, single source, small catchment size areas (Leary et al., 2016; Thomas et al., 2016; Leary et al., 2020b). Accordingly, we narrow our consideration of the major potential source terranes to the southwestern Laurentian continent and focus on nearby uplifts that could have exposed 1370 Ma basement rocks during Early-Middle Pennsylvanian time. We cannot rule out the possibility of zircon recycling from lower Paleozoic strata; however, if there was significant recycling, a more cosmopolitan distribution of ages would be expected (Laskowski et al., 2013; Zotto et al., 2020).

Although all spectra presented here are dominated by peaks at 1370 Ma, up to 28% of analyzed grain ages are outside 1430-1300 Ma (Fig. 5B). Of these grains, we attribute 1900 Ma to ~1800 Ma to Penokean sources (Schulz and Cannon, 2007). The ~1800 Ma to ~1655 Ma ages are interpreted to represent grains sourced from the Yavapai-Mazatzal province, NE-SW oriented zones of juvenile crust that cover much of Arizona, New Mexico, and the American midcontinent (Fig. 8; Karlstrom and Bowring, 1988; Whitmeyer and Karlstrom, 2007). Erosion of early Paleozoic strata may have contributed Paleoproterozoic grains to the Morrow B in the Farnsworth Unit (e.g. Amato and Mack, 2012).

Felsic magmatism has been documented along the southeastern margin of Laurentia during the Mesoproterozoic. Basement ages generally young toward the southwest with the youngest basement ages (~1370 Ma) dated in the southern Granite-Rhyolite province in the modern American Southwest (e.g. Van Schmus et al., 1996; Barnes et al., 2002; Bickford et al., 2015). Granitic basement ~100 km southwest of the study area has yielded U-Pb zircon ages of 1341-1400 Ma (Bickford et al., 2015). These ages overlap with 1370 Ma populations in Morrow

B samples (Figs. 1B, 5A, and 8), and we interpret the southern Granite-Rhyolite province rocks as the most likely source of 1370 Ma zircon in the Morrow B.

We interpret 1300-900 Ma grains to have been sourced from Grenville-age rocks (Fig. 5; Rivers, 1997; Heumann et al., 2006; Whitmeyer and Karlstrom, 2007; Gehrels et al., 2011). Grenville-age granites are widespread in the northeastern United States, but similar age rocks are also present in the Llano Uplift of central Texas and in isolated plutons in Colorado and New Mexico (Scharer and Allegre, 1982; Bickford et al., 2000; Whitmeyer and Karlstrom, 2007; Mosher et al., 2008). Erosion of early Paleozoic strata may have contributed Grenville-age grains to the Morrow B in the Farnsworth Unit (e.g. Amato and Mack, 2012).

All samples analyzed here contain scattered Paleozoic and Neoproterozoic grains ranging from 646 Ma to 307 Ma (Fig. 5B). Potential sources for these grains include accreted peri-Gondwanan terranes with ages ranging from 800-500 Ma (Thomas et al., 2017), Gondwanan arc with ages from 310-270 Ma (Pereira et al., 2012; Ortega-Obregón et al., 2013), and the Appalachian province with grains from 500-270 Ma (Thomas et al., 2017; Waite et al., 2020) (Fig.8).

5.3 Possible muscovite sources

There are substantially fewer published muscovite ages (basement and detrital) than zircon ages, so provenance interpretations for these data are more speculative. Muscovite data are grouped into three prominent peaks at 1625 Ma, 1370 Ma, and 1230 Ma. The ca. 1625 Ma peak is consistent with derivation from Mazatzal-Yavapai province basement (Karlstrom and Bowring, 1988; Whitmeyer and Karlstrom, 2007); however, in the southwestern USA, Paleoproterozoic muscovite cooling ages are generally sparse and limited to geographically restricted regions (Shaw et al., 2005). This is primarily due to the substantial thermal overprinting related to 1.4 Ga magmatism and the Picuris Orogeny (Daniel et al., 2013). The majority of rocks containing Paleoproterozoic muscovite crop out in central Arizona, the Grand Canyon area, and small pockets in New Mexico and Colorado (Shaw et al., 2005; Mulder et al., 2017). Basement exposed in the South Dakota Black Hills region also yields Paleoproterozoic muscovite cooling ages (Dahl and Foland, 2008) and could represent a source.

The 1230 Ma muscovite age peak overlaps with Grenville basement ages (Rivers, 1997; Bickford et al., 2000; Heumann et al., 2006; Whitmeyer and Karlstrom, 2007; Gehrels et al., 2011), and we interpret Grenville rocks to have been the source for these grains.

The 1370 Ma muscovite population corresponds to the dominant zircon population of the same age in all samples presented here. We interpret muscovite grains of this age to have been sourced from the same 1370 Ma granites that supplied 1370 Ma zircon to the study area or from surrounding muscovite bearing country rock in which muscovite was reset by 1370 Ma magmatism. Muscovite bearing rocks have been described in the Granite-Rhyolite province (Ham et al., 1965; Van Schmus et al., 1996) including leucogranites in the Texas Panhandle (Barnes et al., 2002). Although zircon and muscovite have different closure temperatures, >800°C and 400°C, respectively (Lee et al., 1997; Harrison et al., 2009), granites in the southern Granite-Rhyolite province have been interpreted as epizonal--emplaced within a few kilometers of the surface (Thomas et al., 1984). Such granites would crystallize above muscovite's argon closure temperature in normal continental crust (Barbier, 2002); however, their shallow emplacement would facilitate rapid cooling and would result in similar zircon and muscovite ages.

5.4 Morrow B sediment provenance

Based on detrital zircon and muscovite geochronologic data presented here, we evaluate three potential provenance scenarios for the Morrow B sandstone: sourcing from the Ancestral Front Range Uplift northwest of the study area, the Sierra Grande Uplift west of the study area, or the Amarillo Uplift directly south of the study area (Figs. 1 and 9).

The Ancestral Front Range has been a known contributor of Yavapai-Mazatzal and Mesoproterozoic age detritus to adjacent sedimentary basins beginning in the Atokan (Bashkirian-Moscovian) sAge (Leary et al., 2020b). Therefore, the newly calculated Desmoinesian (Moscovian-Kasimovian) Age maximum depositional age overlaps with delivery of 1100 Ma zircons to the Denver Basin during the Desmoinesian (Moscovian-Kasimovian) (Leary et al., 2020b). It is possible that the Morrow B received sediment from the Ancestral Front Range Uplift via southeast-flowing fluvial systems documented in eastern Colorado (Bowen and Weimer, 2003; Puckett et al., 2008). Sourcing of Grenville-age grains from the northeastern United States is unlikely due to their distance from the study area (Leary et al., 2020b); however, we cannot rule the northern Appalachians out as a potential source. The Llano province could also have contributed Grenville-age grains, but these rocks were exposed to the south of the Amarillo-Wichita Uplift (e.g.Whitmeyer and Karlstrom, 2007), which would likely have blocked their transport into the Anadarko Basin (Fig. 1). Therefore, we interpret the most likely source for the Grenville-age zircon grains in this provenance scenario to have been Grenville rocks that were exposed in the Ancestral Front Range (e.g. the Pikes Peak batholith). However, ages in our samples that are consistent with Ancestral Front Range sources make up only a small amount of our overall age population in the Morrow B, and 1370 Ma ages are not abundant in Ancestral Front Range detritus shed into the Denver Basin during the Atokan (Bashkirian-Moscovian) (Leary et al., 2020b). Therefore, although we cannot definitively rule out the Ancestral Front Range as a source, we argue that the data are more consistent with the Ancestral Front Range providing only minor volumes of sediment (see below).

The Sierra Grande Uplift is located in northeastern New Mexico, southeastern Colorado, and the Texas Panhandle (Fig. 1) and is defined by a zero isopach of Pennsylvanian strata (McKee and Crosby, 1975). The Sierra Grande Uplift includes parts of the southern Granite-Rhyolite province and contains basement ages that overlap with the 1370 Ma peak in Morrow B samples (Fig. 1B and 5; Bickford et al., 2015). Basement rocks were likely exposed at the surface in the Sierra Grande Uplift by Atokan-Desmoinesian (Bashkirian-Kasimovian) time (Brotherton et al., 2019) and could have been a source for the Morrow B. In the Tucumcari Basin, directly south of the Sierra Grande Uplift, Broadhead and King (1988) interpreted minor sedimentation beginning in Atokan (Bashkirian-Moscovian) time, with more voluminous, arkosic, deposition beginning during the Desmoinesian (Moscovian-Kasimovian) (Brotherton et al., 2019). McCasland (1980) shows granite wash shed off the Sierra Grande Uplift as restricted to the proximal portion of the Palo Duro Basin, and it seems unlikely that such material would have entered the Anadarko Basin. To the north, the north-south trending Cimarron Uplift likely served as a topographic high during the Desmoinesian (Moscovian-Kasimovian) and separated the Dalhart Basin from the Anadarko Basin (e.g. Fig. 1; McKee and Crosby, 1975; Dutton et al., 1979). Such a topographic high would have blocked sediment from entering the Anadarko Basin. Therefore, we argue that the Sierra Grande Uplift was not a contributor of 1370 Ma sediment to the Morrow B in the Farnsworth Unit.

Published U-Pb zircon ages from the Amarillo-Wichita Uplift are ~550-525 Ma from rocks emplaced in the Southern Oklahoma Aulacogen (Ham et al., 1965; Thomas et al., 2016; Wall et al., 2020). However, these ages come from surface exposures in the Wichita segment of the uplift located in southeastern Oklahoma, ~250 km southeast of the current study area (Fig. 1). Basement rocks of the Amarillo segment of the Amarillo-Wichita Uplift have been dated only from select well cores/cuttings. Ages in the Amarillo segment (western side) of the Amarillo-Wichita Uplift are 1341-1400 Ma (Fig. 1B; Bickford et al., 2015) and overlap with the primary Morrow B age peak at 1370 Ma (Fig. 5A). Although muscovites from these samples have not been dated, we argue that epizonal emplacement of these plutons (Thomas et al., 1984) would result in similar $^{40}Ar/^{39}Ar$ muscovite and U-Pb zircon ages (see above). Basement was exposed in the Amarillo Uplift during the Atokan (Bashkirian-Moscovian) (Dutton, 1982; Johnson, 1989). Atokan (Bashkirian-Moscovian) basement exposure, close proximity to the study area, and close overlap in basement ages make the Amarillo Uplift our preferred primary source area for the Morrow B within the Farnsworth Unit.

5.5 Implications for Anadarko Basin sediment provenance

Previous studies of the Lower Pennsylvanian stratigraphy in the northwest Anadarko Basin have suggested sedimentation by southeast-flowing extrabasinal river systems (Bowen and Weimer, 2003; Puckett et al., 2008). The Morrow B in the study area has previously been interpreted either as part of this system (Puckett et al., 2008; Gallagher, 2014) or as part of a system draining the Amarillo-Wichita Uplift to the south (Munson, 1989). The data presented here suggest that basement rocks in the Amarillo Uplift were exposed at the surface and shedding sediment into the Anadarko Basin by the early Desmoinesian (Moscovian) and that the interface between proximal Amarillo Uplift sediment and more distal sediment transported into the basin via southeast flowing rivers was northeast of the Farnsworth Unit, which is consistent with the interpretations of Bowen and Weimer (2003) (Fig. 9). This revised provenance interpretation for the Morrow B does not necessarily change the depositional model of the

Morrow B as an incised fluvial deposit (e.g. Gallagher, 2014; Rose-Coss, 2017); however, it suggests that the Morrow B in the Farnsworth Unit is part of an overall northeastward flowing fluvial system, which is consistent with paleocurrent data from Rose-Coss (2017), even if the part of this system preserved in the Farnsworth Unit is locally northwest-southeast oriented (Fig. 9) as has been previously reported (Gallagher, 2014; Rose-Coss, 2017).

Whereas we interpret the Amarillo Uplift as the primary source for the Morrow B, the erosion of Amarillo Uplift rocks does not provide a source for Proterozoic grains outside the 1430-1300 Ma range and Paleozoic grains that are present in all samples presented here. There are several possibilities for the provenance of these grains (see above), but we favor a model in which these grains were transported into the Anadarko Basin by southeast-flowing fluvial systems draining the Ancestral Rocky Mountains and American midcontinent and then mixed with proximal Amarillo Uplift detritus by longshore currents during highstand conditions (Fig. 9). During the highstand that deposited the lower member of the Morrow Shale--stratigraphically below the Morrow B (Fig. 2)--the Farnsworth Unit would have been flooded, and longshore currents could have introduced grains sourced from the Ancestral Rocky Mountains or American midcontinent to shoreline sediments (Fig. 9). During the following sea-level fall and lowstand, these shoreline sediments could have been reworked and incorporated into the Morrow B sandstone. In this scenario, the majority of grains would be sourced from the Amarillo Uplift to the south, with a smaller number of grains coming from the Ancestral Rocky Mountains or midcontinent sources. Although longshore current mixing during highstand is our preferred model, we also cannot rule out eolian transport of non-1430-1300 Ma grains into the Anadarko Basin (M. Soreghan et al., 2008; G. Soreghan et al., 2014).

5.6 Implications for detrital provenance studies

Recent work has shown that reliance on a single mineral for detrital provenance studies may not capture all detrital sources due to variable zircon fertility (Moecher and Samson, 2006), sediment recycling (e.g. Zotto et al., 2020), hydraulic sorting (Garzanti, 2016), pebble abrasion (Lavarini et al., 2018), or differences in mineral closure temperatures (Copeland et al., 1990; Mulder et al., 2017). This study relies on geochronology of two detrital minerals with nearly opposite end-member hydraulic properties (Garzanti et al., 2008; Resentini et al., 2013) and disparate closure temperatures, zircon: >800°C; muscovite: 400°C, (Lee et al., 1997; Harrison et al., 2009).

Several features emerge from this combined dataset that serve as examples of the interpretive power of multiple mineral systems in detrital provenance studies. First, despite the different closure temperatures and hydrodynamic properties of the two minerals, the Yavapai-Mazatzal, the Granite-Rhyolite province, and the Grenville-age grains are present in both datasets (Fig. 5). However, their relative proportions are substantially different between zircon and muscovite datasets. Zircon age spectra contain >50% ~1370 Ma grains, whereas the muscovite spectrum is trimodally distributed between these age groups (Fig. 5). We interpret this to reflect muscovite's higher susceptibility to tractive transport compared to zircon (Garzanti et al., 2008; Resentini et al., 2013; Augustsson et al., 2019). If highstand longshore currents were the dominant mode of Ancestral Rocky Mountains sediment transport into the Farnsworth Unit, muscovite may have been more mobile than zircon, resulting in a more even distribution between Ancestral Rocky Mountain and Amarillo Uplift sourced grains. Conversely, different relative abundances of muscovite and zircon in source rocks could also account for the observed differences in relative abundances of muscovite and zircon in the age spectra. The combination of two detrital minerals allows for a more comprehensive provenance interpretation for the

Morrow B. It should be noted however, that we dated substantially more zircons from each sample compared to muscovite crystals, and larger muscovite datasets are necessary to fully compare these two datasets.

Second, the data presented here provide an interesting example of the potential power to distinguish sources with different emplacement/cooling histories. The close overlap in zircon and muscovite ages at ~1370 Ma may indicate that plutons from which these grains were sourced were emplaced at relatively shallow crustal levels if both zircons and muscovites of this age share the same provenance. If Mesoproterozic plutons in the Amarillo Uplift were emplaced at mid-crustal depths, we would expect significant differences between zircon and muscovite ages as is common in the present day Precambrian rocks of the Rocky Mountain region (e.g. Karlstrom et al., 1997; Shaw et al., 2005). Although dating of muscovite from Amarillo Uplift basement samples, and better provenance constraint in general, would be required to fully test this idea, coupled zircon-muscovite provenance data may be a valuable tool in identifying epizonal igneous sources in the sedimentary record.

6. Conclusions

We present U-Pb detrital zircon data for three samples and detrital muscovite $^{40}Ar/^{39}Ar$ data for one sample from the Middle Pennsylvanian Morrow B sandstone in the subsurface Anadarko Basin. Based on these results, we draw the following conclusions:

1. We establish a new maximum depositional age of 310.9 ± 4.9 Ma based on a weighted mean of the youngest concordant zircon grains (3 grains) in sample 13-14-7715. This changes the age of the Morrow B to Desmoinesian (Moscovian) stage.

2. Based on nearly unimodal zircon populations at 1370 Ma, a similar detrital muscovite age peak, and previously interpreted epizonal emplacement of granites in the Amarillo Uplift, we conclude that the Amarillo Uplift in the Texas Panhandle was the primary source for Morrow B detritus.
3. Based on minor abundances of Yavapai-Mazatzal and Grenville-age grains, we argue that small volumes of sediment sourced from the Ancestral Front Range or American midcontinent were incorporated into the Morrow B in the Farnsworth Unit via axial fluvial transport into the northwest Anadarko Basin and longshore current along highstand coastline(s).
4. Geochronological provenance datasets that include multiple minerals provide greater interpretive power than single mineral datasets because they may offset the effects of selective transport, differential mineral fertility, and differential resistance to weathering. Here, a multi-mineral dataset provides additional provenance constraints based on previously interpreted emplacement depths of igneous source areas and sheds light on sediment transport processes.

Acknowledgements

Funding for this project is provided by the U.S. Department of Energy's (DOE) National Energy Technology Laboratory (NETL) through the Southwest Regional Partnership on Carbon Sequestration (SWP) under Award No. DE-FC26-05NT42591. We would like to the thank the staff of New Mexico Bureau of Geology & Mineral Resources, the Arizona LaserChron lab, and Zirchron LLC for their help with sample preparation and analysis. The ideas presented in this paper were improved upon by discussion with Noah Hobbs and Ron Broadhead. We would also like to thank Tim Lawton, Branimir Segvic, Xiangyang Xie, and Drustin Sweet for careful reviews that improved the quality of this manuscript; additional thanks to Dustin Sweet for editorial handling of this manuscript.

References

Alsalem, O.B., Fan, M., Zamora, J., Xie, X., Griffin, W.R., 2017. Paleozoic sediment dispersal before and during the collision between Laurentia and Gondwana in the Fort Worth Basin, USA. Geosphere 14, 325-342.

Amato, J.M., Mack, G.H., 2012. Detrital zircon geochronology from the Cambrian-Ordovician Bliss Sandstone, New Mexico: Evidence for contrasting Grenville-age and Cambrian sources on opposite sides of the Transcontinental Arch. Geological Society of America Bulletin 124, 1826-1840.

Ampomah, W., Balch, R., Cather, M., Rose-Coss, D., Dai, Z., Heath, J., Dewers, T., Mozley, P., 2016. Evaluation of CO2Storage Mechanisms in CO2Enhanced Oil Recovery Sites: Application to Morrow Sandstone Reservoir. Energy & Fuels 30, 8545-8555.

Augustsson, C., Aehnelt, M., Voigt, T., Kunkel, C., Meyer, M., Schellhorn, F., Plink-Björklund, P., 2019. Quartz and zircon decoupling in sandstone: Petrography and quartz cathodoluminescence of the Early Triassic continental Buntsandstein Group in Germany. Sedimentology 66, 2874-2893.

Barbier, E., 2002. Geothermal energy technology and current status: an overview. Renewable & Sustainable Energy Reviews 6, 3-65.

Barnes, M.A., Anthony, E.Y., Williams, I., Asquith, G.B., 2002. Architecture of a 1.38-1.34 Ga granite-rhyolite complex as revealed by geochronology and isotopic and elemental geochemistry of subsurface samples from west Texas, USA. Precambrian Research 119, 9-43.

Benowitz, J.A., Davis, K., Roeske, S., 2019. A river runs through it both ways across time: 40Ar/39Ar detrital and bedrock muscovite geochronology constraints on the Neogene paleodrainage history of the Nenana River system, Alaska Range. Geosphere 15, 682-701.

Bickford, M.E., Soegaard, K., Nielsen, K.C., Mclellend, J.M., 2000. Geology and geochronology of Grenville-age rocks in the Vanhorn and Franklin Mountains area, west Texas: Implications for the tectonic evolution of Laurentia during the Grenville. GSA Bulletin 112, 1134-1148.

Bickford, M.E., Van Schmus, W.R., Karlstrom, K.E., Mueller, P.A., Kamenov, G.D., 2015. Mesoproterozoic-trans-Laurentian magmatism: A synthesis of continent-wide age distributions, new SIMS U–Pb ages, zircon saturation temperatures, and Hf and Nd isotopic compositions. Precambrian Research 265, 286-312.

Blum, M., Pecha, M., 2014. Mid-Cretaceous to Paleocene North American drainage reorganization from detrital zircons. Geology 42, 607-610.

Bowen, D.W., Weimer, P., 2003. Regional sequence stratigraphic setting and reservoir geology of Morrow incised-valley sandstones (lower Pennsylvanian), eastern Colorado and western Kansas. AAPG Bulletin 87, 781-815.

Boyd, D., 2008. Stratigraphic guide to Oklahoma oil and gas reservoirs. Oklahoma Geological Survey

Broadhead, R.F., King, W.E., 1988. Petroleum geology of Pennsylvanian and Lower Permian strata, Tucumcari Basin, east-central New Mexico. New Mexico Bureau of Mines & Mineral Resources Bulletin 119, 1-81.
Brotherton, J.L., Chowdhury, N.U.M.K., Sweet, D.E., 2019. A Synthesis of Late Paleozoic Sedimentation in Central and Eastern New Mexico: Implicaiton for Timing of ANcestral ROcky Mountains Deformation. Society for Sedimentary Geology.
Budnik, R.T., 1986. Left-lateral intraplate deformation along the Ancestral Rocky Mountains: implications for late Paleozoic plate motions. Tectonophysics 132, 195-214.
Cather, S.M., Heizler, M.T., Williamson, T.E., 2019. Laramide fluvial evolution of the San Juan Basin, New Mexico and Colorado: Paleocurrent and detrital-sanidine age constraints from the Paleocene Nacimiento and Animas formations. Geosphere 15, 1641-1664.
Copeland, P., Harrison, T.M., Heizler, M.T., 1990. 40Ar/39Ar Single-Crystal Dating of Detrital Muscovite and K-Feldspar from Let 116, Southern Bengal Fan: Implications for the Uplift and Erosion of the Himalayas. Proceedings of the Ocean Drilling Program, Scientific Results 116, 93-114.
Dahl, P.S., Foland, K.A., 2008. Concentric slow cooling of a low-P-high-T terrane: Evidence from 1600-1300 Ma mica dates in the 1780-1700 Ma Black Hills Orogen, South Dakota, U.S.A. American Mineralogist 93, 1215-1229.
Daniel, C.G., Pfeifer, L.S., Jones, J.V., McFarlane, C.M., 2013. Detrital zircon evidence for non-Laurentian provenance, Mesoproterozoic (ca. 1490-1450 Ma) deposition and orogenesis in a reconstructed orogenic belt, northern New Mexico, USA: Defining the Picuris orogeny. Geological Society of America Bulletin 125, 1423-1441.
Dickinson, W.R., Lawton, T.F., 2001. Carboniferous to Cretaceous assembly and fragmentation of Mexico. GSA Bulletin 113, 1142-1160.
Dickinson, W.R., Lawton, T.F., 2003. Sequential intercontinental suturing as the ultimate control for Pennsylvanian Ancestral Rocky Mountains deformation. Geology 31.
Domeier, M., Torsvik, T.H., 2014. Plate tectonics in the late Paleozoic. Geoscience Frontiers 5, 303-350.
Dutton, S.P., 1982. Pennsylvanian Fan-Delta and Carbonate Deposition, Mobeetie Field, Texas Panhandle. AAPG Bulletin 66, 389-407.
Dutton, S.P., Finley, R.J., Galloway, W.E., Gustavson, T.C., Handford, C.R., Presley, M.W., 1979. Geology and Geohydrology of the Palo Duro Basin, Texas Panhandle. Geological Circular 79-1, 1-99.
Feinstein, S., 1981. Subsidence and Thermal History of Southern Oklahoma Aulacogen: Implications for Petroleum Exploration. AAPG Bulletin 65, 2521-2533.
Gallagher, S.R., 2014. Depositional and Diagenetic Controls on Reservoir Heterogeneity: Upper Morrow Sandstoen, Farnsworth Unit, Ochiltree County, Texas. New Mexico Institute of Mining and Technology, 1-214.
Garzanti, E., 2016. From static to dynamic provenance analysis—Sedimentary petrology upgraded. Sedimentary Geology 336, 3-13.
Garzanti, E., Andò, S., Vezzoli, G., 2008. Settling equivalence of detrital minerals and grain-size dependence of sediment composition. Earth and Planetary Science Letters 273, 138-151.
Gehrels, G., Pecha, M., 2014. Detrital zircon U-Pb geochronology and Hf isotope geochemistry of Paleozoic and Triassic passive margin strata of western North America. Geosphere 10, 49-65.

Gehrels, G., Valencia, V.A., Pullen, A., 2006. Detrital Zircon Geochronology by Laser-Ablation Multicollector ICPMS at the Arizona Laserchron Center. Geochronology: Emerging Opportunites, Paleontology Society Short Course: Palentology Society Papers 12.
Gehrels, G.E., Blakey, R., Karlstrom, K.E., Timmons, J.M., Dickinson, B., Pecha, M., 2011. Detrital zircon U-Pb geochronology of Paleozoic strata in the Grand Canyon, Arizona. Lithosphere 3, 183-200.
Gehrels, G.E., Valencia, V.A., Ruiz, J., 2008. Enhanced precision, accuracy, efficiency, and spatial resolution of U-Pb ages by laser ablation-multicollector-inductively coupled plasma-mass spectrometry. Geochemistry, Geophysics, Geosystems 9, n/a-n/a.
Graham, S.A., Dickinson, W.R., Ingersoll, R.V., 1975. Himalayan-Bengal Model for Flysch Dispersal in the Appalachian-Ouachita System. Geological Society of America Bulletin 86.
Gutiérrez-Alonso, G., Fernández-Suárez, J., Collins, A.S., Abad, I., Nieto, F., 2005. Amazonian Mesoproterozoic basement in the core of the Ibero-Armorican Arc: 40Ar/39Ar detrital mica ages complement the zircon's tale. Geology 33.
Ham, W.E., Denison, R.E., Merritt, C.A., 1965. Basement Rocks and Structural Evolution of Southern Oklahoma-A Summary. AAPG Bulletin 49, 927-934.
Harrison, T.M., Célérier, J., Aikman, A.B., Hermann, J., Heizler, M.T., 2009. Diffusion of 40Ar in muscovite. Geochimica et Cosmochimica Acta 73, 1039-1051.
Heckel, P.H., 2008. Pennsylvanian Cyclothems in Midcontinent North America as far-field effects of waxing and waning of Gondwana ice sheets. Geological Society of America Bulletin, 275-289.
Heumann, M.J., Bickford, M.E., Hill, B.M., McLelland, J.M., Selleck, B.W., Jercinovic, M.J., 2006. Timing of anatexis in metapelites from the Adirondack lowlands and southern highlands: A manifestation of the Shawinigan orogeny and subsequent anorthosite-mangerite-charnockite-granite magmatism. Geological Society of America Bulletin 118, 1283-1298.
Johnson, K.S., 1989. Geologic Evolution of the Anadarko Basin Oklahoma Geological Survey Circular 90, 3-12.
Karlstrom, K.E., Bowring, S.A., 1988. Early Proterozoic Assembly of Tectonostratigraphic Terranes in Southwestern North America. The Journal of Geology 96, 561-576.
Karlstrom, K.E., Dallmeyer, R.D., Grambling, J.A., 1997. 40Ar/39Ar Evidence for 1.4 Ga Regional Metamorphism in New Mexico: Implications for Thermal Evolution of Lithosphere in the Southwestern USA. The Journal of Geology 105, 205-223.
Keller, G.R., Stephenson, R.A., 2007. The Southern Oklahoma and Dniepr-Donets aulacogens: A comparative analysis, 4-D Framework of Continental Crust, pp. 127-143.
Kluth, C.F., Coney, P.J., 1981. Plate tectonics of the Ancestral Rocky Mountains. Geology 9, 10-15.
Kuiper, K.F., Deino, A., Hilgen, F.J., Krijgsman, W., Renne, P.R., Wijbrans, J.R., 2008. Synchronizing rock clocks of Earth history. Science 320, 500-504.
Laskowski, A.K., DeCelles, P.G., Gehrels, G.E., 2013. Detrital zircon geochronology of Cordilleran retroarc foreland basin strata, western North America. Tectonics 32, 1027-1048.
Lavarini, C., Attal, M., da Costa Filho, C.A., Kirstein, L.A., 2018. Does Pebble Abrasion Influence Detrital Age Population Statistics? A Numerical Investigation of Natural Data Sets. Journal of Geophysical Research: Earth Surface 123, 2577-2601.

Leary, R., Orme, D.A., Laskowski, A.K., DeCelles, P.G., Kapp, P., Carrapa, B., Dettinger, M., 2016. Along-strike diachroneity in deposition of the Kailas Formation in central southern Tibet: Implications for Indian slab dynamics. Geosphere 12, 1198-1223.
Leary, R.J., Smith, M.E., Umhoefer, P., 2020a. Grain-Size Control on Detrital Zircon Cycloprovenance in the Late Paleozoic Paradox and Eagle Basins, USA. Journal of Geophysical Research: Solid Earth 125.
Leary, R.J., Umhoefer, P., Smith, M.E., Riggs, N., 2017. A three-sided orogen: A new tectonic model for Ancestral Rocky Mountain uplift and basin development. Geology.
Leary, R.J., Umhoefer, P., Smith, M.E., Smith, T.M., Saylor, J.E., Riggs, N., Burr, G., Lodes, E., Foley, D., Licht, A., Mueller, M.A., Baird, C., 2020b. Provenance of Pennsylvanian–Permian sedimentary rocks associated with the Ancestral Rocky Mountains orogeny in southwestern Laurentia: Implications for continental-scale Laurentian sediment transport systems. Lithosphere 12, 88-121.
Lee, J.K.W., Williams, I.S., Ellis, D.J., 1997. Pb, U and Th diffusion in natural zircon. Nature 390, 159-162.
Lee, W., 1953. Subsurface gologic cross section from Meade County to Smith County, Kansas. United States Geological Survey, 23.
Li, Z.X., Bogdanova, S.V., Collins, A.S., Davidson, A., De Waele, B., Ernst, R.E., Fitzsimons, I.C.W., Fuck, R.A., Gladkochub, D.P., Jacobs, J., Karlstrom, K.E., Lu, S., Natapov, L.M., Pease, V., Pisarevsky, S.A., Thrane, K., Vernikovsky, V., 2008. Assembly, configuration, and break-up history of Rodinia: A synthesis. Precambrian Research 160, 179-210.
Ludwig, K.R., 2003. User's manual for Isoplot 3.75: A Geochronologic Toolkit for Microsoft Excel (No. 5).
Maher, J.C., 1948. Subsurface geologic cross section from Baca County to Yuma County, Colorado. United States Geological Survey, 11.
Mallory, W.W., 1972. Pennsylvanian system: Regional synthesis. Geologic Atlas of the Rocky Mountain Region Rocky Mountain Association of Geologists, 111-127.
Marshak, S., Karlstrom, K.E., Timmons, J.M., 2000. Inversion of Proterozoic extensional faults: An explanation for the pattern of Laramide and Ancestral Rockies intracratonic deformation, United States. Geology 28, 735-738.
McCasland, R.D., 1980. Subsurface Geology of the Dalhard Basin, Texas Panhandle. Texas Tech University, 1-147.
McKee, E.D., Crosby, E.J., 1975. Paleotectonic Investigations of the Pennsylvanian System in the United States. U.S. Geological Survey Professional Paper 853.
McKee, E.D., McKee, S.S., 1967. Paleotectonic maps of the Permian System. U.S. Geological Survey IMAP 450.
Merriam, D.F., 1963. The Geologic History of Kansas. Kansas Geological Survey Buelletin 162.
Min, K., Mundil, R., Renne, P.R., Ludwig, K.R., 2000. A test for systematic errors in $^{40}Ar/^{39}Ar$ geochronology through comparison with U/Pb analysis of 1.1-Ga rhyolite. Geochimica et Cosmochimica Acta 64, 73-98.
Moecher, D., Samson, S., 2006. Differential zircon fertility of source terranes and natural bias in the detrital zircon record: Implications for sedimentary provenance analysis. Earth and Planetary Science Letters 247, 252-266.
Mosher, S., Levine, J.S.F., Carlson, W.D., 2008. Mesoproterozoic plate tectonics: A collisional model for the Grenville-aged orogenic belt in the Llano uplift, central Texas. Geology 36.

Mulder, J.A., Karlstrom, K.E., Fletcher, K., Heizler, M.T., Timmons, J.M., Crossey, L.J., Gehrels, G.E., Pecha, M., 2017. The syn-orogenic sedimentary record of the Grenville Orogeny in southwest Laurentia. Precambrian Research 294, 33-52.

Munson, T.W., 1989. Depositional, Diagenetic, and Production History of the Upper Morrowan Buckhaults Sandstone, Farnsworth Field, Ochiltree County Texas. Shale Shaker Digest 40, 2-19.

Ortega-Obregón, C., Solari, L., Gómez-Tuena, A., Elías-Herrera, M., Ortega-Gutiérrez, F., Macías-Romo, C., 2013. Permian–Carboniferous arc magmatism in southern Mexico: U–Pb dating, trace element and Hf isotopic evidence on zircons of earliest subduction beneath the western margin of Gondwana. International Journal of Earth Sciences 103, 1287-1300.

Pereira, M.F., Chichorro, M., Johnston, S.T., Gutiérrez-Alonso, G., Silva, J.B., Linnemann, U., Hofmann, M., Drost, K., 2012. The missing Rheic Ocean magmatic arcs: Provenance analysis of Late Paleozoic sedimentary clastic rocks of SW Iberia. Gondwana Research 22, 882-891.

Perry, W., J. Jr., 1989. Tectonic Evolution of the Anadarko Basin Region, Oklahoma. U.S. Geological Survey Bulletin 1866-A, 1-19.

Puckett, J., Al-Shaieb, Z., Van Evera, E., 2008. Sequence Stratigraphy, Lithofacies, and Reservoir Quality, Upper Morrow Sandstones, Northwestern Shelf, Anadarko Basin. Oklahoma Geological Survey Circular 111, 81-97.

Rascoe, B.J., Adler, F.J., 1983. Permo-Carboniferous Hydrocarbon Accumulations, Mid-Continent, U.S.A. AAPG Bulletin 67, 979-1001.

Repasch, M., Karlstrom, K., Heizler, M., Pecha, M., 2017. Birth and evolution of the Rio Grande fluvial system in the past 8 Ma: Progressive downward integration and the influence of tectonics, volcanism, and climate. Earth-Science Reviews 168, 113-164.

Resentini, A., Malusà, M.G., Garzanti, E., 2013. MinSORTING: An Excel® worksheet for modelling mineral grain-size distribution in sediments, with application to detrital geochronology and provenance studies. Computers & Geosciences 59, 90-97.

Richards, B.C., 2013. Current status fo the international Carboniferous time scale. The Carboniferous-Permian Transition, New Mexico Museum of Natural Histroy and Science, Bulletin, 348-352.

Rivers, T., 1997. Lithotectonic elements of the Grenville Province: review and tectonic implications. Precambrian Research 86, 117-154.

Rose-Coss, D., 2017. A Refined Depositional Sequence Stratigraphic and Structural Model for the Reservoir and Caprock Intervals at the Farnsworth Unit, Ochiltree County TX. New Mexico Institute of Mining and Technology 1-231.

Ross, C.A., 1986. Paleozoic evolution of southern margin of Permian basin. GSA Bulletin 97, 536-554.

Ross, C.A., Ross, J.R.P., 1987. Late Paleozoic Sea Levels and Depositional Sequences. Cushman Foundation for Foraminiferal Research 24, 137-149.

Scharer, U., Allegre, C.J., 1982. Uranium-lead system in fragments of a single zircon. Nature, 585-587.

Schulz, K.J., Cannon, W.F., 2007. The Penokean orogeny in the Lake Superior region. Precambrian Research 157, 4-25.

Scotese, C.R., Boucot, A.J., McKerrow, W.S., 1999. Gondwanana Palaeogeography and Palaeoclimatology. Journal of African Earth Sciences 28, 99-114.

Shaw, C.A., Heizler, M.T., Karlstrom, K.E., 2005. 40Ar/39Ar thermochronologic record of 1.45–1.35 Ga intracontinental tectonism in the southern Rocky Mountains: Interplay of conductive and advective heating with intracontinental deformation, The Rocky Mountain Region—An Evolving Lithosphere: Tectonics, Geochemistry, and Geophysics, pp. 163-184.

Soreghan, G., Keller, G.R., Gilbert, M.C., Chase, C.G., Sweet, D.E., 2012. Load-induced subsidence of the Ancestral Rocky Mountains recorded by preseration of Permain landscapes. Geosphere 8.

Soreghan, G.S., Sweet, D.E., Heavens, N.G., 2014. Upland Glaciation in Tropical Pangaea: Geologic Evidence and Implications for Late Paleozoic Climate Modeling. The Journal of Geology 122, 137-163.

Soreghan, M.J., Soreghan, G.S., Hamilton, M.A., 2008. Glacial–interglacial shifts in atmospheric circulation of western tropical Pangaea. Palaeogeography, Palaeoclimatology, Palaeoecology 268, 260-272.

Thomas, J.J., Shuster, R.D., Bickford, M.E., 1984. A terrane of 1,350- to 1,400-m.y.-old silicic volcanic and plutonic rocks in the buried Proterozoic of the mid-continent in the wet mountains, Colorado. GSA Bulletin 95, 1150-1157.

Thomas, W.A., Gehrels, G.E., Greb, S.F., Nadon, G.C., Satkoski, A.M., Romero, M.C., 2017. Detrital zircons and sediment dispersal in the Appalachian foreland. Geosphere 13, 2206-2230.

Thomas, W.A., Gehrels, G.E., Lawton, T.F., Satterfield, J.I., Romero, M.C., Sundell, K.E., 2019. Detrital zircons and sediment dispersal from the Coahuila terrane of northern Mexico into the Marathon foreland of the southern Midcontinent. Geosphere 15, 1102-1127.

Thomas, W.A., Gehrels, G.E., Romero, M.C., 2016. Detrital zircons from crystalline rocks along the Southern Oklahoma fault system, Wichita and Arbuckle Mountains, USA. Geosphere 12, 1224-1234.

Van Schmus, W.R., Bickford, M.E., Turek, A., 1996. Proterozoic geology of the east-central Midcontinent basement. Geological Society of America Special Paper 308, 7-32.

Wahlman, G.P., 2013. Pennsylvanian to Lower Permian (Desmoinesian-Wolfcampian) fusulinid biostratigraphy of Mid continent North America. Stratigraphy 10, 73-104.

Waite, L., Fan, M., Collins, D., Gehrels, G., Stern, R.J., 2020. Detrital zircon provenance evidence for an early Permian longitudinal river flowing into the Midland Basin of west Texas. International Geology Review 62, 1224-1244.

Wall, C.J., Hanson, R.E., Schmitz, M., Price, J.D., Donovan, R.N., Boro, J.R., Eschberger, A.M., Toews, C.E., 2020. Integrating zircon trace-element geochemistry and high-precision U-Pb zircon geochronology to resolve the timing and petrogenesis of the late Ediacaran–Cambrian Wichita igneous province, Southern Oklahoma Aulacogen, USA. Geology 49.

Whitmeyer, S.J., Karlstrom, K.E., 2007. Tectonic model for the Proteroxoic growth of North America. Geosphere 3, 220-259.

Ye, H., Royden, L., Burchfiel, C., Schuepbach, M., 1996. Late Paleozoic Deformation of Interior North America: The Greater Ancestral Rocky Mountains. AAPG Bulletin 80, 1397-1432.

Zotto, S.C., Moecher, D.P., Niemi, N.A., Thigpen, J.R., Samson, S.D., 2020. Persistence of Grenvillian dominance in Laurentian detrital zircon age systematics explained by sedimentary recycling: Evidence from detrital zircon double dating and detrital monazite textures and geochronology. Geology 48, 792-797.

Table 1. Well and core data.

Well name	Latitude	Longitude	Location of core	Core length
13-10A	36.3651	-101.01061	New Mexico Bureau of Geology & Mineral Resources	~80 m (260 ft)
13-14	36.26264	-101.00598	New Mexico Bureau of Geology & Mineral Resources	~83 m (270 ft)
32-8	36.242406	-100.95036	New Mexico Bureau of Geology & Mineral Resources	~78 m (255 ft)

Figure 1. (A) Map of Midcontinent late Paleozoic tectonic elements after Merriam (1963); McKee and McKee (1967); Mallory (1972); McKee and Crosby (1975); Dutton et al. (1979); Leary et al. (2020b). Basins: Ad – Anadarko, Pd – Palo Duro, Dh – Dalhart, Cc – Central Colorado Trough, Ea – Eagle, Px – Paradox, Dv – Denver, Tu – Tucumcari. Major and minor uplift designation from Soreghan et al. (2012) and Leary et al. (2020b). Major uplifts: Am – Amarillo, Wi – Wichita, Sg – Sierra Grande, Fr – Ancestral Front Range, Uu – Uncompahgre. Minor uplifts: Ck – Central Kansas, Cm – Cimarron, Pe – Pedernal, Ma – Matador Arch, and La – Las Animas Arche. (B) Enlarged view of rectangle from figure 1A, showing U-Pb ages of basement rocks, taken from the subsurface, in millions of years (Bickford et al., 2015).

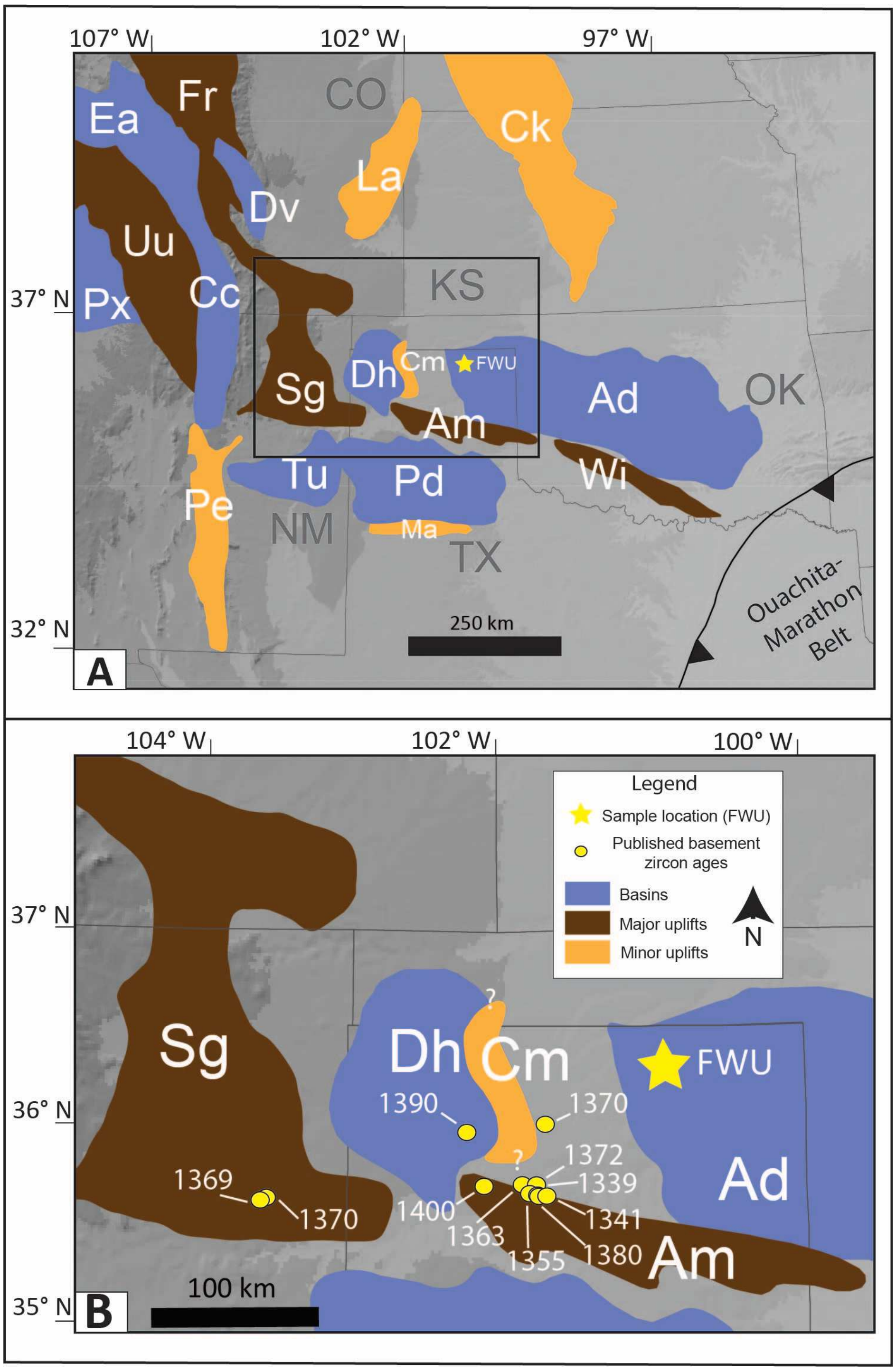
107° W
102° W
97° W
37° N
32° N
CO
KS
OK
NM
TX
Ea
Fr
Dv
La
Ck
Uu
Cc
Px
Sg
Dh
Cm
FWU
Ad
Am
Wi
Tu
Pd
Pe
Ma
250 km
Ouachita-
Marathon
Belt
A
104° W
102° W
100° W
36° N
35° N
Legend
Sample location (FWU)
Published basement
zircon ages
Basins
Major uplifts
Minor uplifts
N
1390
1370
1372
1339
1341
1380
1355
1363
1400
1369
100 km
B

Figure 2. General stratigraphic column of the Anadarko Basin after Boyd (2008) and Munson (1989). Timescale after Richards (2013).

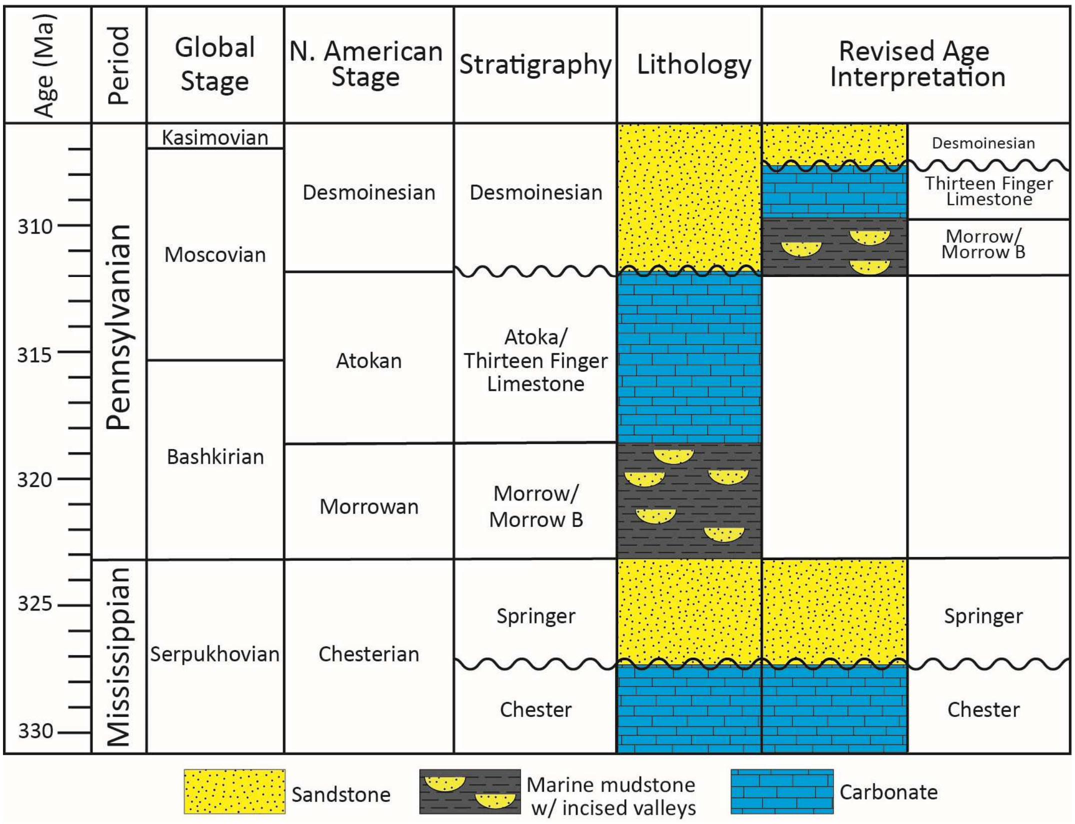

Figure 3. Location of cores (stars) at the Farnsworth Unit, north Texas. Black outline is the outline of the Farnsworth Unit oil and gas field. Description of core modified from (Rose-Coss, 2017) showing facies associations and locations of zircon and muscovite samples.

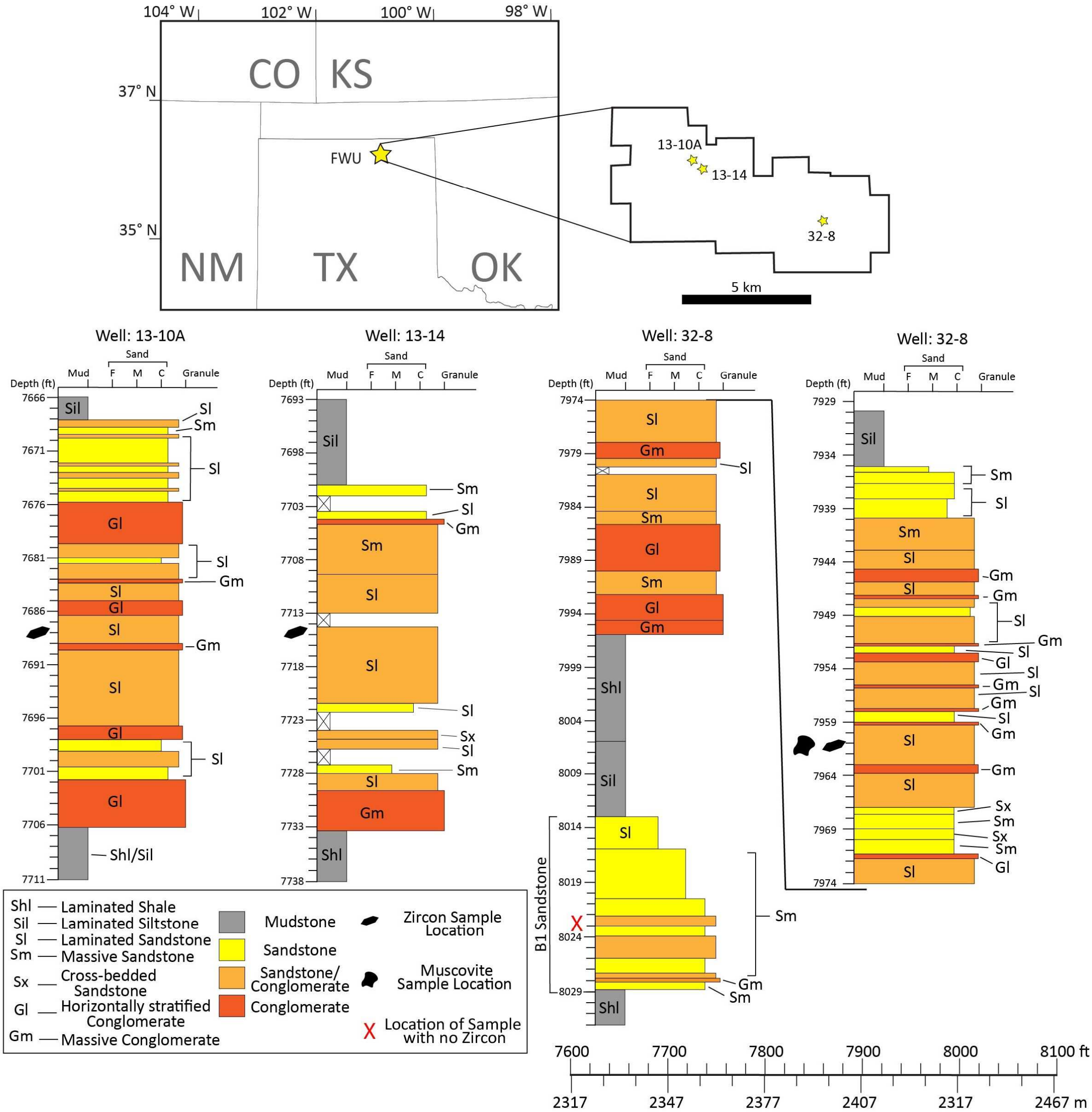

Figure 4. Core photos taken from the Farnsworth Unit, TX. Numbers on the core are depth in ft. (A) from core 13-10A, showing sharp contact between underlying siltstone and mudstone with the basal conglomerate of the Morrow B. (B) From core 13-14 showing coarse to granular sandstone/conglomerate and finer grained laminated facies with stylolites and clay drapes (bottom). (C) From core 32-8 showing cross bedded facies (top).

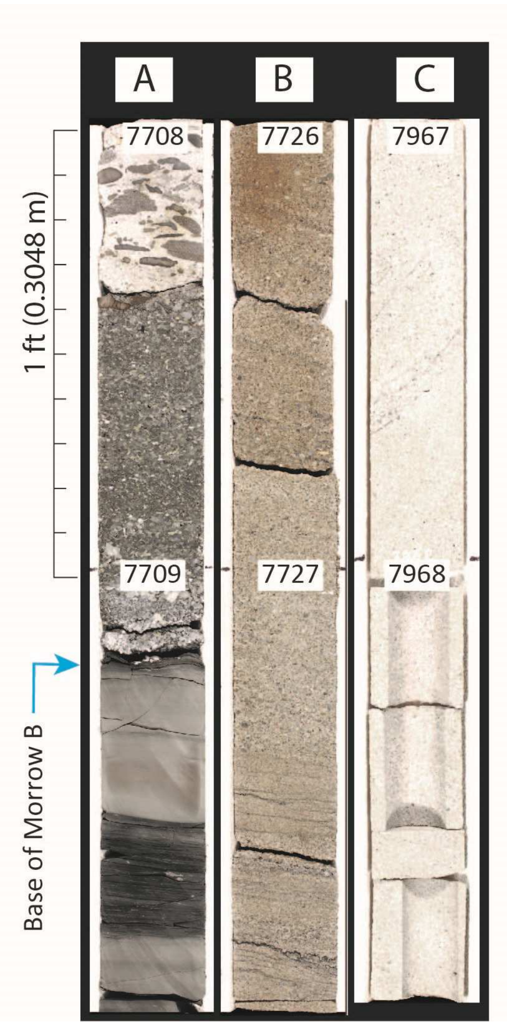

Figure 5. U-Pb detrital zircon and $^{40}Ar/^{39}Ar$ detrital muscovite results from 3 samples; 13-10A-7688, 13-14-7715, and 32-8-7961. Results are displayed in both probability density plots and kernel density estimates. Bandwidth for kernel density estimate is 20 Ma and bin width for histogram is 50 Ma. The y-axis illustrates maximums for histograms. (A) Age spectrum of all zircon and muscovite results. (B) Age spectrum of zircon and muscovite without 1300-1400 Ma ages, in order to better visualize ages outside primary 1370 Ma peak.

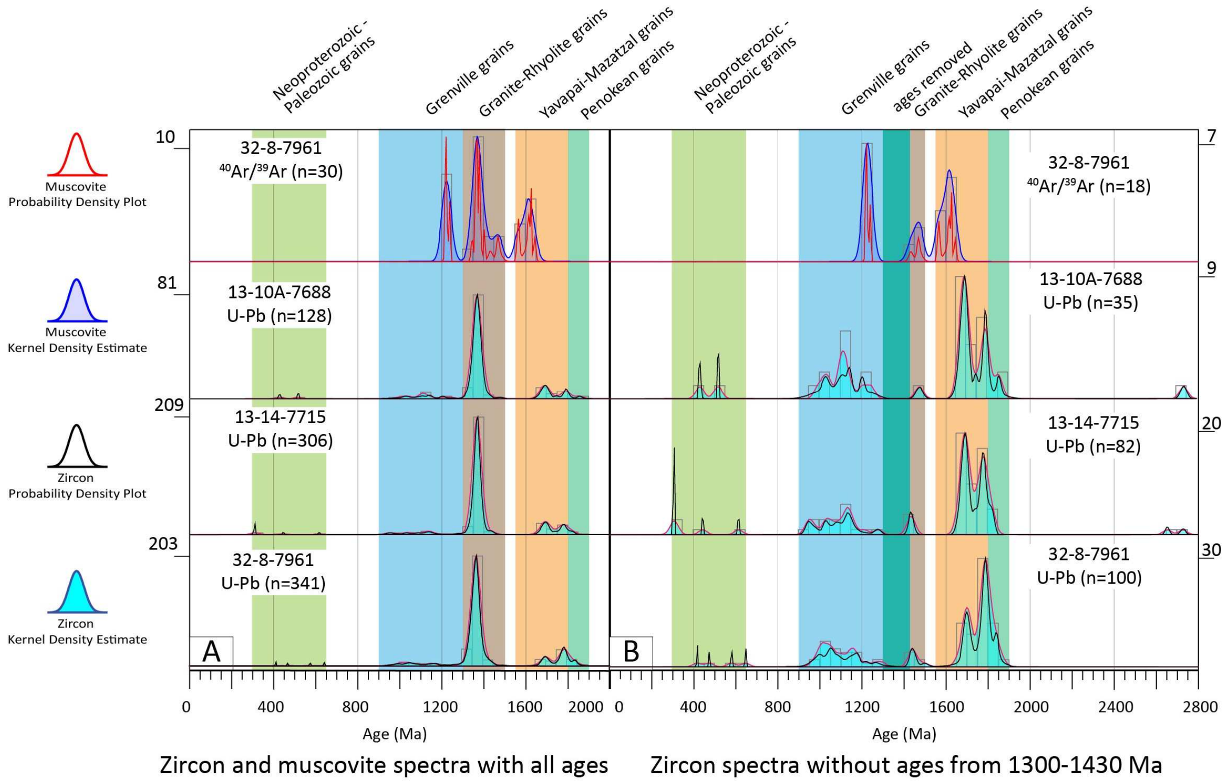

Figure 6. New maximum depositional age of 310.9±4.9 Ma (including systematic error) for sample 13-14-7715 calculated using weighted average for the youngest age peak. Red bars are 1σ uncertainty.

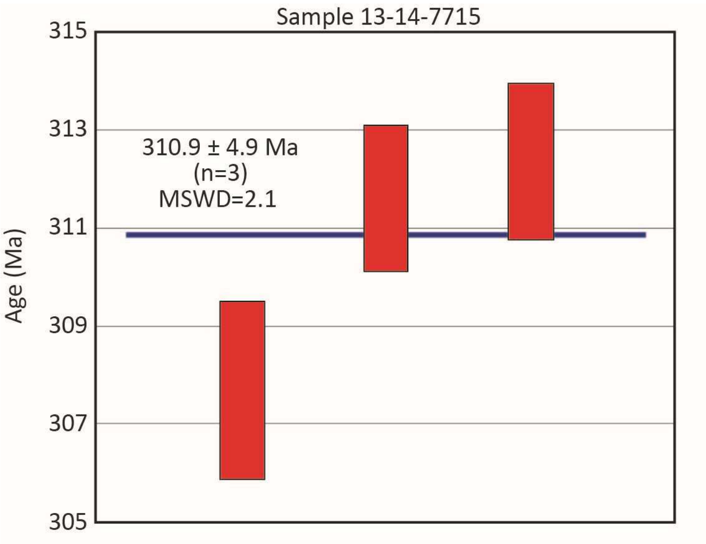

Figure 7. Step heating analysis and plateau definition of muscovite crystals.

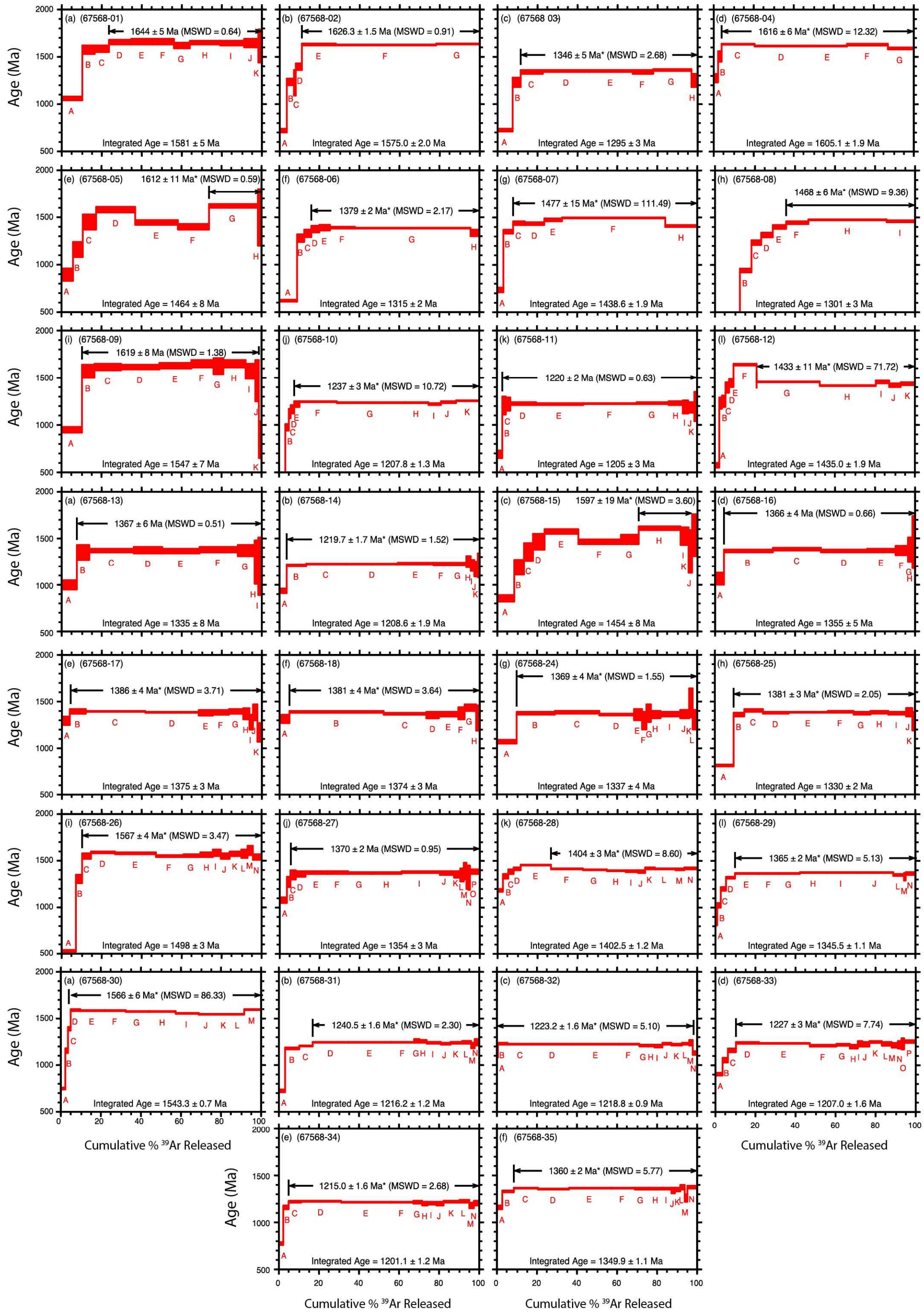

Age (Ma)
(a) (67568-01)
1644 ± 5 Ma (MSWD = 0.64)
Integrated Age = 1581 ± 5 Ma
(b) (67568-02)
1626.3 ± 1.5 Ma (MSWD = 0.91)
Integrated Age = 1575.0 ± 2.0 Ma
(c) (67568 03)
1346 ± 5 Ma* (MSWD = 2.68)
Integrated Age = 1295 ± 3 Ma
(d) (67568-04)
1616 ± 6 Ma* (MSWD = 12.32)
Integrated Age = 1605.1 ± 1.9 Ma
(e) (67568-05)
1612 ± 11 Ma* (MSWD = 0.59)
Integrated Age = 1464 ± 8 Ma
(f) (67568-06)
1379 ± 2 Ma* (MSWD = 2.17)
Integrated Age = 1315 ± 2 Ma
(g) (67568-07)
1477 ± 15 Ma* (MSWD = 111.49)
Integrated Age = 1438.6 ± 1.9 Ma
(h) (67568-08)
1468 ± 6 Ma* (MSWD = 9.36)
Integrated Age = 1301 ± 3 Ma
(i) (67568-09)
1619 ± 8 Ma (MSWD = 1.38)
Integrated Age = 1547 ± 7 Ma
(j) (67568-10)
1237 ± 3 Ma* (MSWD = 10.72)
Integrated Age = 1207.8 ± 1.3 Ma
(k) (67568-11)
1220 ± 2 Ma (MSWD = 0.63)
Integrated Age = 1205 ± 3 Ma
(l) (67568-12)
1433 ± 11 Ma* (MSWD = 71.72)
Integrated Age = 1435.0 ± 1.9 Ma
(a) (67568-13)
1367 ± 6 Ma (MSWD = 0.51)
Integrated Age = 1335 ± 8 Ma
(b) (67568-14)
1219.7 ± 1.7 Ma* (MSWD = 1.52)
Integrated Age = 1208.6 ± 1.9 Ma
(c) (67568-15)
1597 ± 19 Ma* (MSWD = 3.60)
Integrated Age = 1454 ± 8 Ma
(d) (67568-16)
1366 ± 4 Ma (MSWD = 0.66)
Integrated Age = 1355 ± 5 Ma
(e) (67568-17)
1386 ± 4 Ma* (MSWD = 3.71)
Integrated Age = 1375 ± 3 Ma
(f) (67568-18)
1381 ± 4 Ma* (MSWD = 3.64)
Integrated Age = 1374 ± 3 Ma
(g) (67568-24)
1369 ± 4 Ma* (MSWD = 1.55)
Integrated Age = 1337 ± 4 Ma
(h) (67568-25)
1381 ± 3 Ma* (MSWD = 2.05)
Integrated Age = 1330 ± 2 Ma
(i) (67568-26)
1567 ± 4 Ma* (MSWD = 3.47)
Integrated Age = 1498 ± 3 Ma
(j) (67568-27)
1370 ± 2 Ma (MSWD = 0.95)
Integrated Age = 1354 ± 3 Ma
(k) (67568-28)
1404 ± 3 Ma* (MSWD = 8.60)
Integrated Age = 1402.5 ± 1.2 Ma
(l) (67568-29)
1365 ± 2 Ma* (MSWD = 5.13)
Integrated Age = 1345.5 ± 1.1 Ma
(a) (67568-30)
1566 ± 6 Ma* (MSWD = 86.33)
Integrated Age = 1543.3 ± 0.7 Ma
(b) (67568-31)
1240.5 ± 1.6 Ma* (MSWD = 2.30)
Integrated Age = 1216.2 ± 1.2 Ma
(c) (67568-32)
1223.2 ± 1.6 Ma* (MSWD = 5.10)
Integrated Age = 1218.8 ± 0.9 Ma
(d) (67568-33)
1227 ± 3 Ma* (MSWD = 7.74)
Integrated Age = 1207.0 ± 1.6 Ma
(e) (67568-34)
1215.0 ± 1.6 Ma* (MSWD = 2.68)
Integrated Age = 1201.1 ± 1.2 Ma
(f) (67568-35)
1360 ± 2 Ma* (MSWD = 5.77)
Integrated Age = 1349.9 ± 1.1 Ma
Cumulative % 39Ar Released

Figure 8. North American basement provinces and ages based on (Whitmeyer and Karlstrom, 2007; Gehrels et al., 2011; Gehrels and Pecha, 2014)Hoffman (1989), Whitmeyer and Karlstrom (2007), Gehrels et al. (2011), and Gehrels and Pecha (2014). Provinces: Mo - Mojave; Wy - Wyoming; MH - Medicine Hat; Su - Superior; TH - Trans-Hudson.

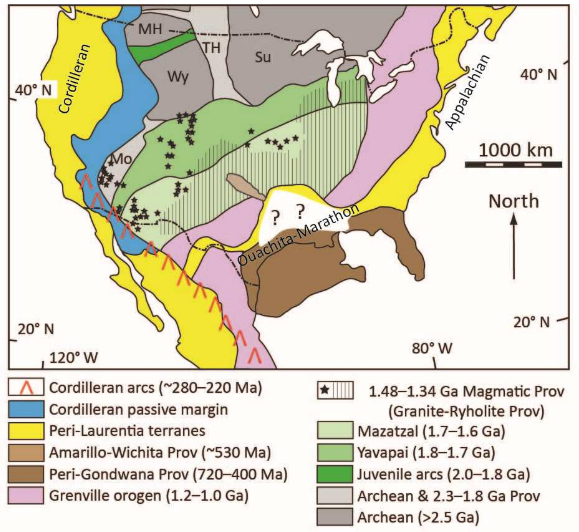

Figure 9. Schematic map of depositional system and tectonic elements during (A) deposition of the Morrow shale at highstand and (B) Morrow B sandstone during lowstand after Merriam (1963); McKee and McKee (1967); (Mallory, 1972); McKee and Crosby (1975); Dutton et al. (1979); Bowen and Weimer (2003); Leary et al. (2020b). Major uplifts: Am – Amarillo, Wi – Wichita, Sg – Sierra Grande, Fr – Ancestral Front Range. Minor uplifts: Ck – Central Kansas and Cm – Cimarron. FWU – Farnsworth Unit.